

Nonlinear behavior of rail fastening system on slab track at railway bridge ends: FEA and experimental study

Deokyong Sung^a, Seongkyu Chang^{b,*}

^a Department of Civil & Railroad Engineering, Daewon University College, 316 Daehak-ro, Jecheon, Chungbuk 27135, Republic of Korea

^b Academic-Industry Cooperation Foundation, Kunsan National University, 558 Daehak-ro, Kunsan, Jeonbuk 54150, Republic of Korea

ARTICLE INFO

Keywords:

Railway bridge
Slab track
Rail fastening system
Nonlinear behavior
Serviceability evaluation method

ABSTRACT

Rail fastening systems on a slab track at railway bridge ends are often damaged, which increases the maintenance costs. The serviceability evaluation of a rail fastening system on a slab track at railway bridge ends is based on the assumption that the stiffness of the rail fastening system is linear. The behavior of the rail fastening system on slab track at the railway bridge ends is studied in detail in this study. In the experimental model, the abutment and pier of the railway bridge were considered to be directly connected to two H-beams through a rail and rail fastening systems. A stiffness model of the rail fastening system for the finite-element analysis was established by performing a clamping-force test. In the finite-element analysis, the rail fastening system was considered as both linear and nonlinear stiffness models. The experimental and numerical results were very similar when the rail fastening system was considered as the nonlinear stiffness model. With the same uplift force acting on the rail fastening system, the displacement results of the nonlinear stiffness model were larger than those of the linear stiffness model. Therefore, it is necessary to employ the nonlinear behavior of the rail fastening system and investigate a displacement-based design method of the rail fastening system when evaluating the serviceability of the rail fastening system on the slab track at railway bridge ends.

1. Introduction

With the exponential growth of high-speed railway (HSR) networks [1–3], construction of railway bridges is constantly increasing. Because bridges are essential parts of HSR infrastructures for crossing valleys, existing train lines, and other obstacles. In addition, the application of slab track systems [4,5] to the railway bridges is constantly increasing. The slab track systems have been developed and implemented in a number of situations, including high-traffic and high-speed lines, in a number of countries. The slab track is being installed to offer increased passenger comfort and require minimal maintenance over time.

In the case of railway bridges with slab tracks, vertical deformation of girders can lead to excessive rail deformation at the bridge ends, which may result in a larger load being applied to the rail fastening systems, which is in contrast to ballasted track systems. The geometric tolerances and tension and compression forces have a significant influence on the design of closed and open bridge joints for slab track [6]. Additionally, in the case of a rail fastening system with high stiffness, a large load is generated in the slab track [7]. These problems at the railway bridge ends need to be more attention as the high-speed lines increase.

To ensure the safety of the slab track at railway bridge ends, criteria [8,9] for evaluating the serviceability of the rail fastening system at the railway bridge slab track ends were proposed. The rotation of the bridge ends enforces a curvature of the slab track in the transition zone [10–12] to the abutment and at the expansion joints on the piers, which additionally stresses the rail fastening system in these areas. These additional stresses [13,14] are called uplift force and compression force and can cause breakage of the fastener clip and plastic deformation of the elastic pad in the rail fastening system of the bridge ends. The serviceability evaluation of the railway bridge ends is classified as rotation and vertical displacement to deformation of the superstructure caused by various loading conditions [8,9]. The force generated in the rail fastening system should be within the range of the initial clamping force of the rail fastener and the limited plastic deformation of the elastic pad. Despite the strict design of rail fastening systems, they are often damaged in the slab track of the railway bridges. The serviceability evaluation of the rail fastening systems at the railway bridge ends are performed in compliance with DS 804 [8] and KR C-08090 [9], under an assumption that the stiffness of the rail fastening system is linear. However, the rail fastening systems exhibit nonlinear behavior [13,14] that can cause a difference between the design and the actual

* Corresponding author.

E-mail address: s9752033@kunsan.ac.kr (S. Chang).

<https://doi.org/10.1016/j.engstruct.2019.05.098>

Received 7 March 2019; Received in revised form 28 May 2019; Accepted 28 May 2019

Available online 04 June 2019

0141-0296/ © 2019 Elsevier Ltd. All rights reserved.

Table 1
Specifications of test specimens.

Component	Model	Unit weight (kg/m)	Length (m)	Number of components
Rail	60KR	60.7	20	1
Rail fastening system	KR-II	–	–	26
H-beam	400X400X13X21	172	10.05	2

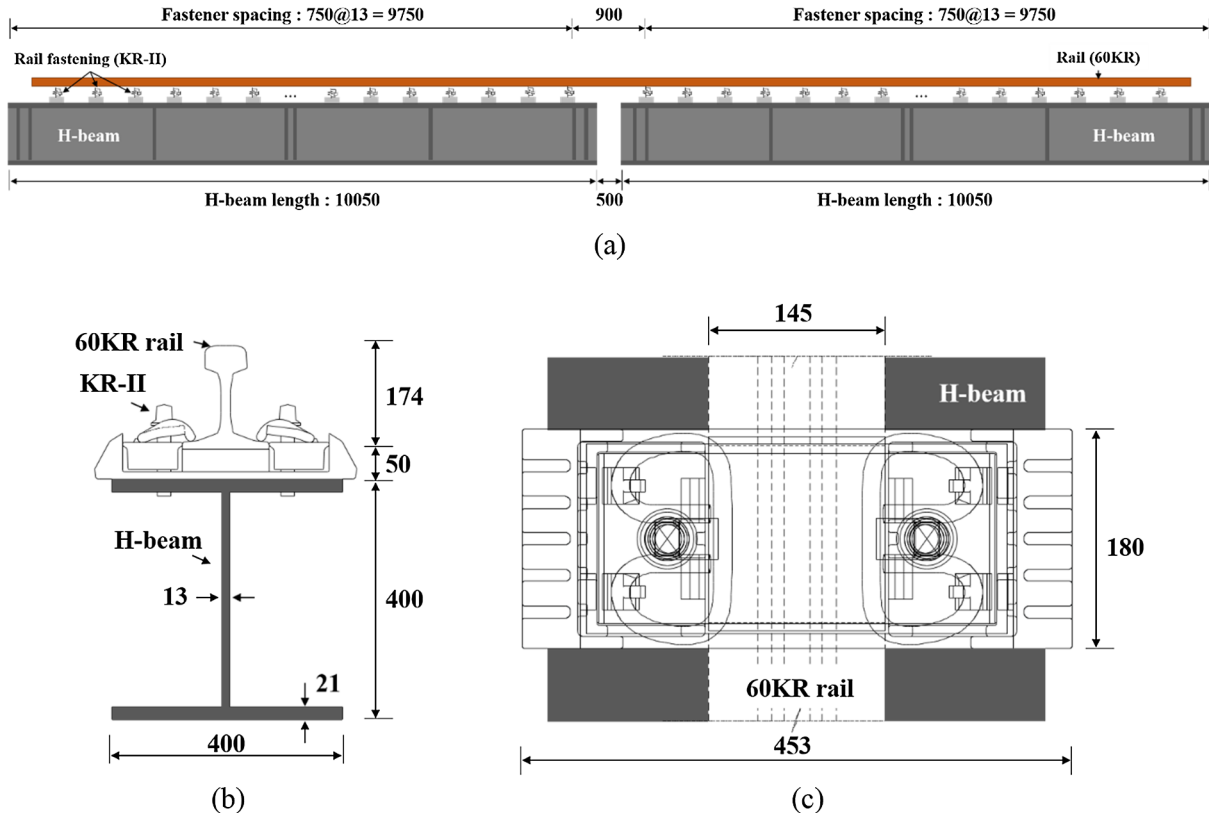


Fig. 1. Design of the test specimens (unit: mm): (a) side view; (b) cross-section; (c) top view of KR-II rail fastening system.

onsite behavior. If the uplift force and compressive force do not satisfy the performance requirements of the serviceability evaluation criteria for the rail fastening system, either a more effective rail fastening system [15] or specialized track system [6,15–17] should be applied. This can increase the cost of building and maintaining the high-speed lines.

Various studies on the railway bridge ends have been performed to ensure the safety of slab tracks and to reduce the maintenance costs of tracks. Moelter [6] noted that there are movements at the end of a superstructure due to deflections of the superstructure and that the longitudinal and lateral displacements can cause high forces in the rail fastening system. Park et al. [18] analyzed the factors influencing the serviceability of the rail fastening system caused by the rotation of support at the railway bridge ends and analyzed the influence degree through a parametric study. According to their experiences in installing slab tracks used in bridges and tunnels, Pichler and Fenske [19] reported the advantages of slab tracks in Australia and Germany when responding to movements and rotations due to interactions between the bridges and tracks at the bridge joints. Choi [20] analyzed the effects of the sleeper spacing and the stiffness of the rail fastening system on the force acting on the sleeper through continuous-support and discrete-support models, which are generally applied for railway track analysis. Choi [21] derived an unequal-spacing discrete-support beam model and analyzed the force of the rail support point according to the distance between the sleepers, and the distance between the bridge bearings and

the last rail fastening system at the bridge ends. Lim et al. [22] investigated the behavior of a slab track induced by rotation of the bridge ends at the ends of the railway bridge.

Recently, various studies [23–31] related to the nonlinear behavior of rail fastening systems and their analytical methods have been conducted. Yang et al. [13] suggested the necessity of a study to consider the nonlinear characteristics of rail fastening devices when evaluating the serviceability of the slab tracks at the railway bridge ends. Sung [14] proposed a nonlinear analysis method for evaluating serviceability of the slab track at railway bridge ends.

The aim of this study is to find out the reason for the breakage of the rail fastening system on the slab track at the railway bridge ends. It is considered that a large upward displacement of the rail is caused by the rotation at the end of the superstructure [6,8,9,14–18]. First, experimental models for the railway bridge ends will be presented. Both an abutment model and a pier model were tested. Afterwards, a finite-element analysis will be carried out to highlight the important factors that influence the upward displacement of the rail fastening system. A clamping-force test for the rail fastening system will be performed to determine the stiffness model for application to the finite-element model. The difference between the linear model and the nonlinear model of the rail fastening system will be indicated. The effect of the distance from the end of the bridge to the center of the bridge support on the forces acting on the rail fastening system will be indicated. Finally, a finite-element modeling method of the rail fastening system will

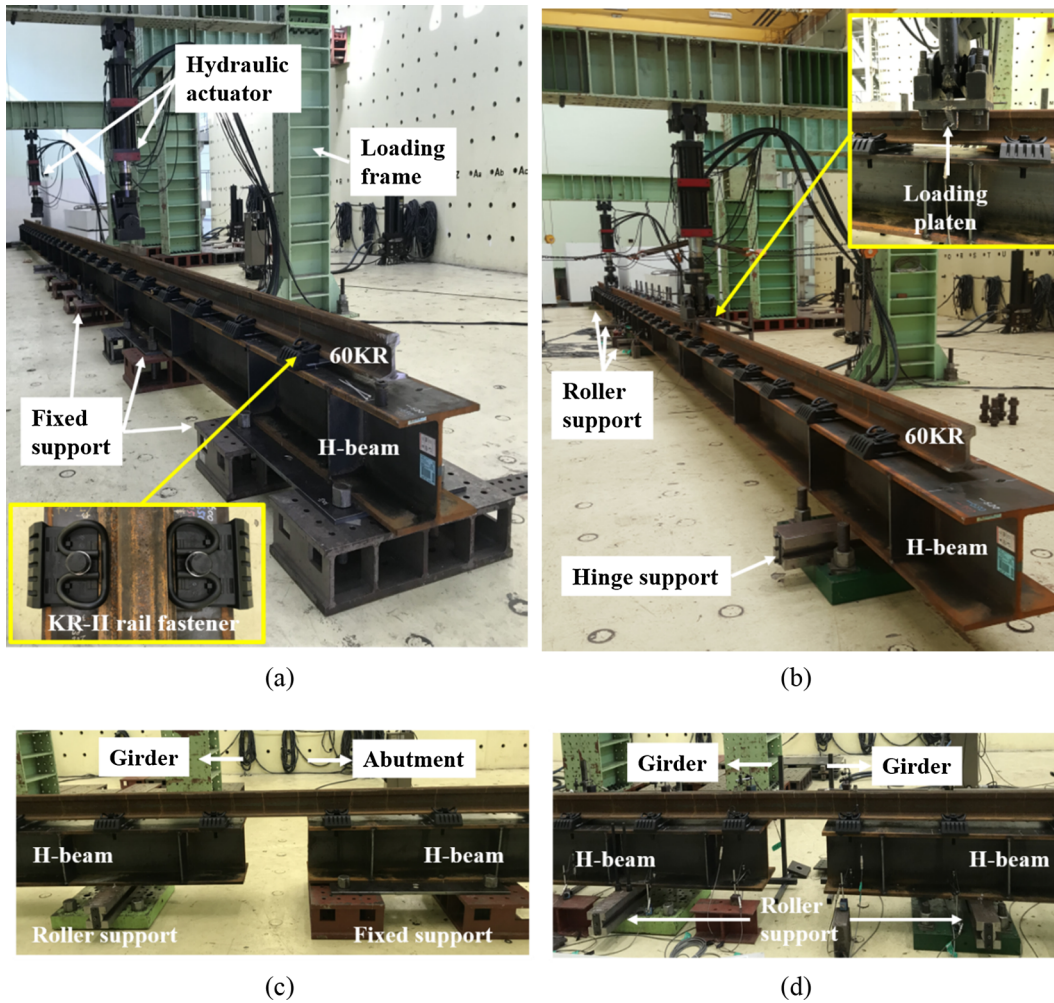


Fig. 2. Overview of the railway bridge model specimens: (a) abutment model; (b) pier model; (c) girder ends in the abutment model; (d) girder ends in the pier model.

Table 2
Cases of the railway bridge model test.

Case	Bearing position (distance from end of girder)	Type of model	Load conditions
Case 1	Boundary condition (1) (950 mm)	Abutment	0–350 kN, 50 kN steps
Case 2	Boundary condition 2 (1135 mm)		0–350 kN, 50 kN steps
Case 3	Boundary condition (1) (950 mm)	Pier	0–300 kN, 50 kN steps (both sides)
Case 4	Boundary condition 2 (1135 mm)		0–300 kN, 50 kN steps (both sides)

be proposed to evaluate the serviceability of the rail fastening system in real railway bridge design.

2. Experimental study

2.1. Test specimens

The current serviceability evaluation method [8,9] of the rail fastening system should calculate the force acting on the rail fastening system by the deformation of the railway bridge ends under unit loads (i.e. unit rotation angle, unit vertical deflection, and unit wheel load). Then, the rotation angles and vertical offsets at the end of the railway bridge deck are calculated for several loads such as the creep and shrinkage, train vertical load, and so on. The final uplift forces acting on

the rail fastening system are calculated using the force by unit load and the deformation of the actual bridge. It is important to calculate the forces acting on the rail fastening system due to the deformation of the railway bridge ends under the various load conditions.

In this study, an experimental model test considering the abutment and pier of railway bridges was performed to investigate the behavior of the rail fastening system at railway bridge ends. Details regarding the experimental model used in this study are presented in Table 1 and Fig. 1. An H-beam [32] was adopted to clarify the behavior of the bridge ends by increasing the girder displacement of the railway bridge. The 60KR rail [33,34] and the KR-II rail fastening system [35–38] were directly connected to the H-beam for transferring the deformation of the end of the girder due to the flexural behavior on the girder. The length of the rail is 20 m. Two H-beams with a length of 10.05 m are

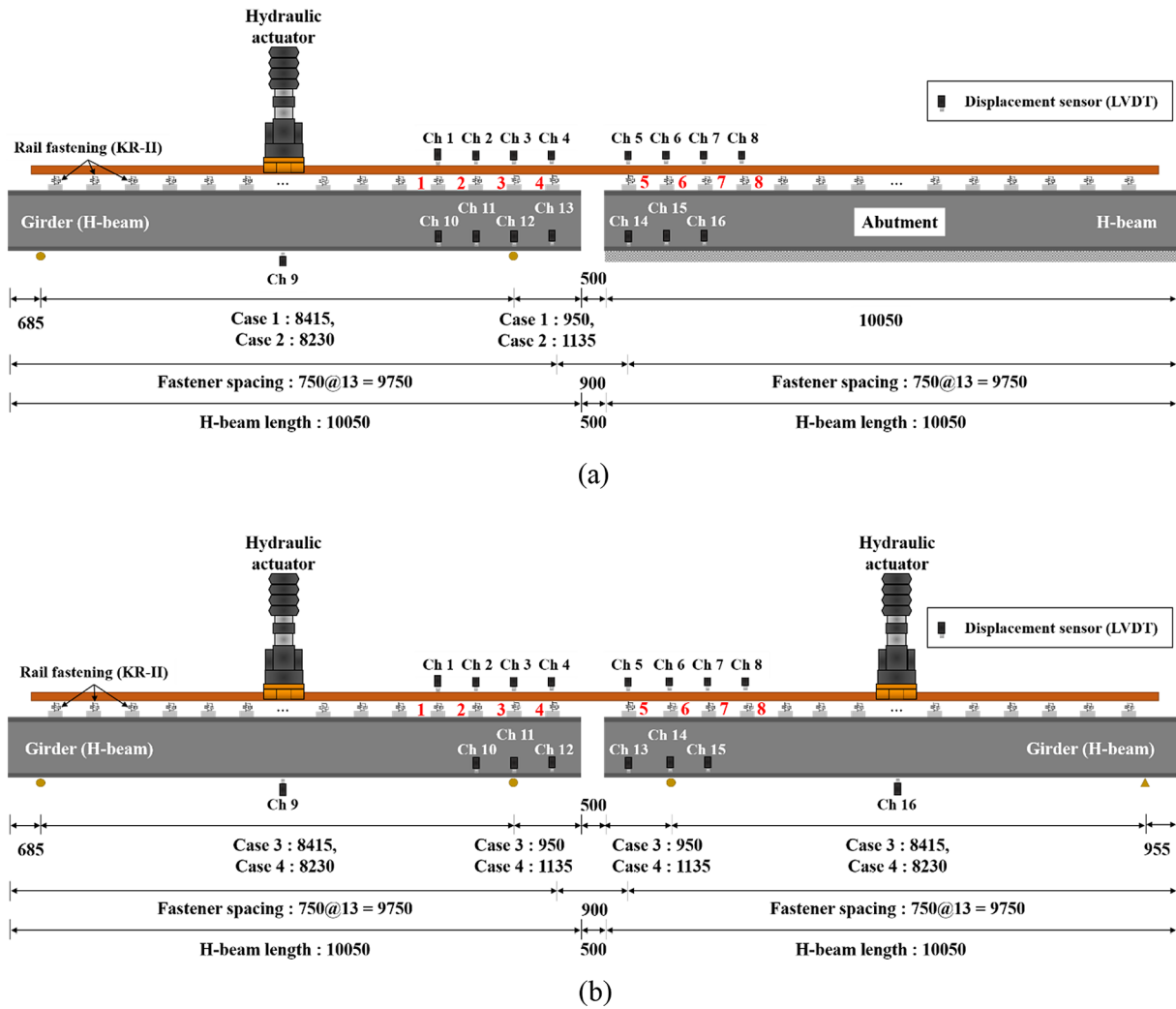


Fig. 3. Loading setup and instrumentation of the railway bridge model (unit: mm): (a) abutment model; (b) pier model.

placed in a straight line. There is a gap of 0.5 m between the H-beams connected by a rail. The rail fastening systems installed on the H-beams are installed at an interval of 0.75 m (see Fig. 1(a)). The height of the specimen, including the rail, the rail fastening system, and the H-beam, is 0.624 m (see Fig. 1(b)). The width of the top specimen is 0.453 m (see Fig. 1(c)).

Fig. 2 shows the railway bridge model specimens. Two railway bridge model specimens were made to simulate the abutment and pier of the railway bridge. In the first specimen, the right H-beam was connected to the bottom to model the abutment of the bridge (see Fig. 2(a) and (c)). In the other specimen, bearings were installed on the right and left sides of the H-beams to consider the pier of the bridge (see Fig. 2(b) and (d)). To increase the girder flexural behavior, the left girder was supported by a roller–roller support. In the case of modeling the bridge pier, only the support point of the right girder ends was used as a hinge support, and all the support points employed roller conditions. The plate that applies the load to the rail is shown in Fig. 2(b).

2.2. Experimental cases and instrumentations

The cases of the railway bridge experimental model are shown in Table 2. Fig. 3 shows the displacement measurement positions and the boundary conditions for each test case. The position of the bearing was

changed according to the test case to confirm the dependence of the rail fastener displacement on the geometrical change of the end of the railway bridge under a static load. In the experimental cases, there are four cases depending on the supporting condition of the right H-beam and the distance from the end of the girder to the center of the bearing. Case 1 and case 2 are the abutment model, and the distances from the end of the girder to the center of the bearing are 950 mm and 1135 mm, respectively (see Fig. 3(a)). Case 3 and case 4 are the pier model, and the distances from the end of the girder to the center of the bearing are 950 mm and 1135 mm, respectively (see Fig. 3(b)). Also, in each case, the distance between the supports of the girder is different.

A hydraulic actuator with a load capacity of 1000 kN was used for the test and was installed at the center of the girder. A force control process was adopted for the test. In the bridge abutment test, the load was increased from 0 to 350 kN with intervals of 50 kN. From the pier of the bridge, the load was applied to both sides of the girder and was increased from 0 to 300 kN. During the test, the increased load is 50 kN at each load step, which was applied with a loading speed of 5 kN/sec. At each load step, the reading was taken manually after the data became stable.

As shown in Fig. 4, displacement-measuring instruments (linear variable differential transformers, LVDTs) were installed to measure the behavior of the end of the railway bridge. The steel frame jig was

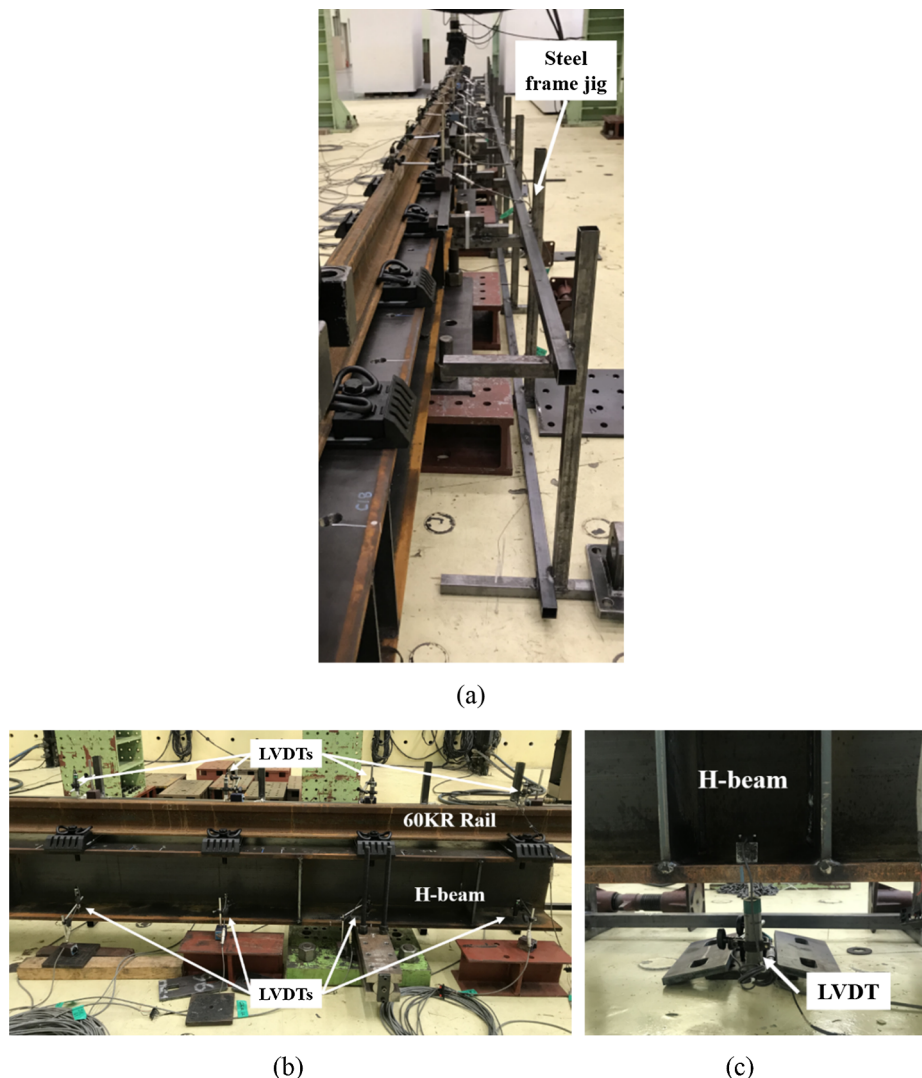


Fig. 4. Overview of LVDT installation: (a) steel frame jig for the installation of the LVDTs; (b) LVDTs installed at the girder ends; (c) LVDT installed at the center of the girder.

prepared so as not to interfere with the measurement of the rail displacement (see Fig. 4(a)). The LVDTs were installed on the rail and girder at the position of the rail fastener (see Fig. 4(b)). To compare the finite-element analysis results with the experimental results, an LVDT was installed at the center of each girder (see Fig. 4(c)). The displacement of the rail and girder at the position of the rail fastener was measured with CDP-10 LVDT [40]. The displacement of the center of each girder was measured with CDP-100 LVDT [40]. The measurement ranges of the CDP-10 and the CDP-100 are ± 5 mm and ± 50 mm, respectively.

3. Finite-element analysis

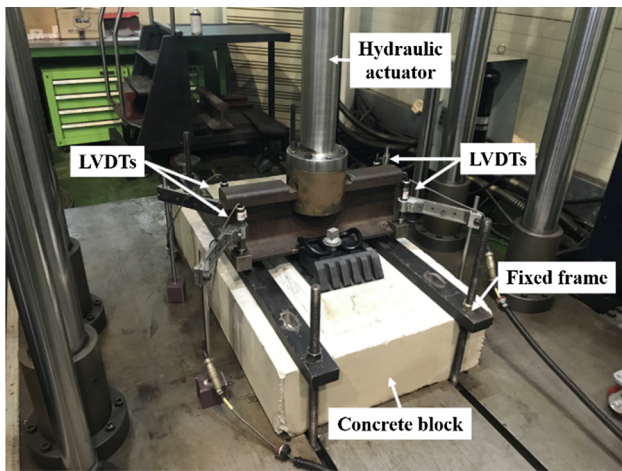
3.1. Numerical model of rail fastening system

Currently, in the serviceability evaluation of the rail fastening system on the slab track at the railway bridge ends, the stiffness of the rail fastener is assumed to be linear [8,9]. In this study, a clamping-

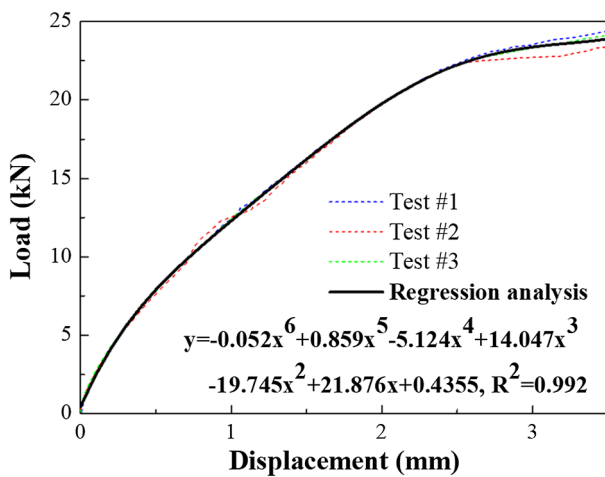
force test [7,14,17,39,42–44] was performed to confirm the actual stiffness of the rail fastening system. The method specified in the Korean Railway Standard [43] and European Standard [44] was employed.

Fig. 5 shows a photograph of the clamping-force test of KR-II rail fastening system [35–38] and its results. The test results were obtained by measuring the displacement at four rail ends when the rail was lifted upwards at a rate of 10 kN/min by installing a rail fastening system on a 0.5 m rail on a fixed concrete block (see Fig. 5(a)). The displacement of the rail was measured with CDP-10 LVDT [40]. Three sets of rail fasteners were prepared to reduce the error, and three clamping-force tests were conducted. The average of the results measured with four LVDTs for each of the three clamping-force tests is shown in Fig. 5(b). In addition, a regression analysis result of three test results is shown.

Fig. 6 shows a comparison between the linear and nonlinear stiffness models of the rail fastening system. The KR-II rail fastening system has a maximum static vertical stiffness value of 30 kN/mm [35,36]. This value indicates the static vertical stiffness due to the compressive



(a)



(b)

Fig. 5. (a) overview of the clamping-force test; (b) load-displacement curve from the clamping-force test.

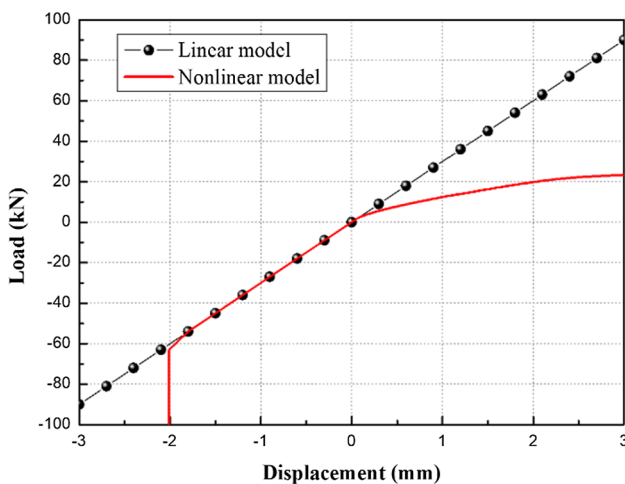


Fig. 6. Stiffness models of the KR-II rail fastening system for finite-element analysis.

load and is applied for the serviceability review of the railway bridge ends [8,9]. In Fig. 6, the maximum static stiffness value according to the conventional method [8,9] was used for the linear model and the average of the three clamping-force test results was used for the nonlinear model. The compression zone represents the stiffness of the rail pad, and the limited compressive displacement of the rail pad is set to 20% of the pad thickness [9,17,35–37] (i.e. 2 mm). Therefore, when the rail fastening system was considered as the nonlinear model, the rail fastener exhibited the nonlinear behavior under the uplift force, and displacement of ≥ 2 mm did not occur under the compressive force.

3.2. Finite-element models (FEMs)

A finite-element analysis was performed to compare the results of the experimental model. The finite-element model was also developed using SAP2000 [41] under the same conditions used in the experimental study. Table 3 presents the properties of the finite-element model. An example of the finite-element models is shown in Fig. 7. The rail and girder were modeled using three-dimensional beam elements. The nonlinear stiffness model of the rail fastening system was simulated using the multi-linear link of SAP2000 [41] with the load–displacement curves shown in Fig. 6. A linear link was used in the linear stiffness model of the rail fastening system, and its stiffness was 30 kN/mm [35,36]. As the vertical displacement occurred on the rollers in the experimental results, the rollers were replaced with a linear link in the simulation. It was necessary to calibrate the displacement results of the girder in the experimental model and in the finite-element model. The stiffness value of the bearing was set via trial and error. The boundary condition was adjusted such that the displacement results of the girder in the experimental model and the finite-element model agreed with each other. The stiffness of the bridge bearings was 250 kN/mm and was identical for both linear and nonlinear stiffness models.

3.3. Model verification

As the first step of the numerical study, the FEMs for the test specimens case 1 and case 3 were developed to verify the numerical method. Fig. 8 shows the displacement results of girder for the experimental model and the numerical model. Fig. 8(a) shows a comparison of the displacement results at the center and the end of the left girder for case 1 under the concentrated load applied at the left girder. Fig. 8(b) shows a comparison of the displacement results at the center and the end of the right girder for case 3 under the concentrated loads applied simultaneously to both girders. The “channel number” shown in Fig. 8 is shown in Fig. 3. In Fig. 8(a), “Ch 9” represents the center displacement of the left girder in the case of the bridge abutment, and in Fig. 8(b), “Ch 16” represents the center displacement of the right girder in the case of the bridge pier. The numerical and experimental values of the vertical displacement are similar at each LVDT location. Therefore, the finite-element models in this study can properly simulate the test specimens and hence can be used to further investigate the behavior of the railway bridge ends.

4. Results and discussion

4.1. Assumption for results analysis

It is difficult to measure the displacement of the rail fastening system directly in the experimental model. The displacement results of the rail fastening system at the end of girder are the results including the displacement of the girder. This is because the displacement is

Table 3
Properties of the girder and track.

		Cross-sectional area (m ²)	Moment of inertia (m ⁴)	Elastic modulus (N/m ²)	Stiffness (kN/mm)	FEM
Rail (60KR)		0.0773	3.064E−5	2.10E+10	–	3-D beam
Rail fastening system (KR-II)	Linear	–	–	–	30 (see Fig. 6)	Linear link
	Nonlinear	–	–	–	See Fig. 6	Multi-linear link
Girder (H-beam)	400 × 400 × 13 × 21 mm	0.0218	6.666E−4	2.091E+10	–	3-D beam
Bridge bearing					250	Linear link

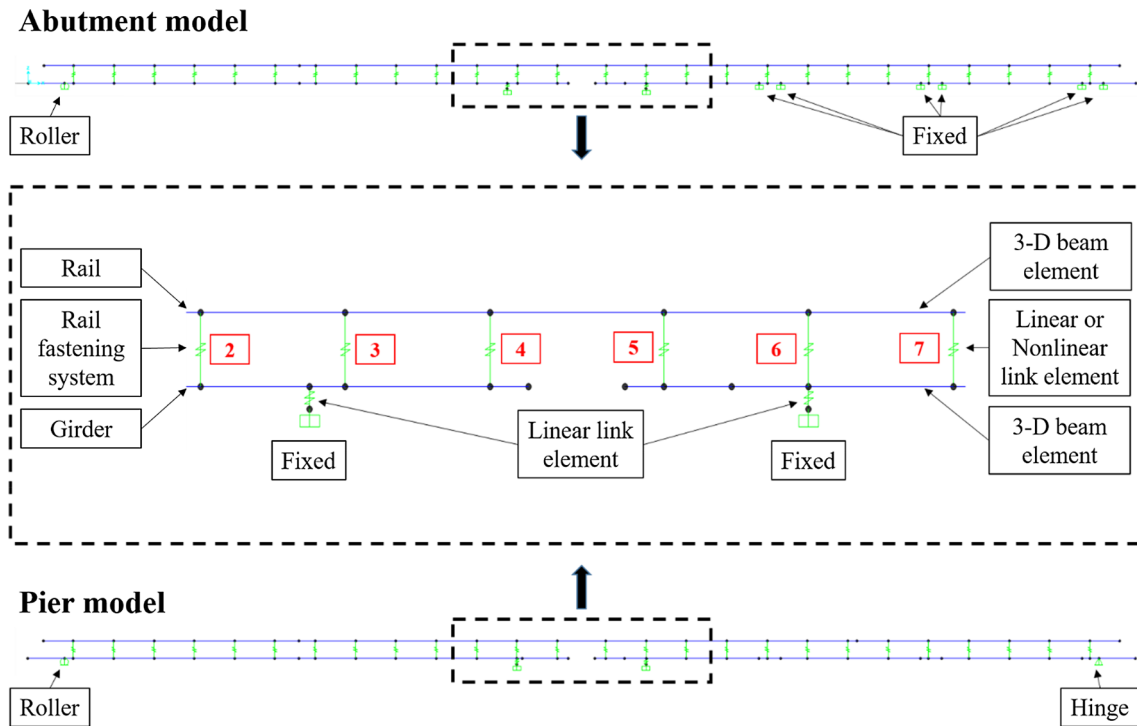


Fig. 7. FEMs of the railway bridge model.

measured through the LVDTs separated from the test specimen. Thus, it is necessary to extract only the displacement results generated in the rail fastening systems by using the displacement measured at the rail and girder.

Fig. 9 shows an assumption to confirm the displacement results of the rail fastening system in the experimental and numerical models. Fig. 9(a) shows the cross section of the experimental model before and after deformation of the bridge ends, and Fig. 9(b) shows its numerical model. In the case, the rail pad and fastener were modeled as a link (green line). A_u and B_u are located in the center of gravity of the rail and girder, respectively. The assumption is that there is no deformation of the girder and the upward displacement occurs in the rail and fastener. In this case, the upward displacement (d_f) of the fastener will be equal to the rail displacement (d_r), which applies equally to both the experimental and the numerical model. Eq. (1) shows a general formula for calculating the displacement of the rail fastening system when deformation occurs in the girder.

$$d_f = d_r = (A_D - A_U) - (B_D - B_U) \quad (1)$$

where d_r and d_f are the displacements of rail and fastener, respectively; A_u and B_u are the measurement points on the rail and girder under the

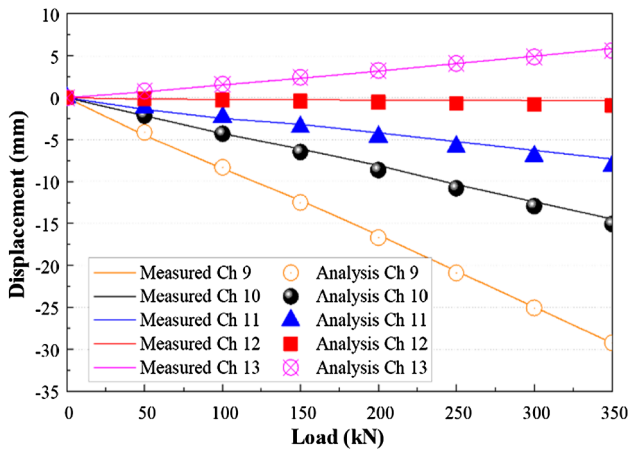
undeformed shape, respectively; A_d and B_d are the measurement points on the rail and girder under the deformed shape, respectively.

If d_f is larger than zero, the rail fastening system is subjected to a tensile force (i.e. upward displacement), and if d_f is smaller than zero, the rail fastening system is subjected to a compressive force (i.e. compressive displacement).

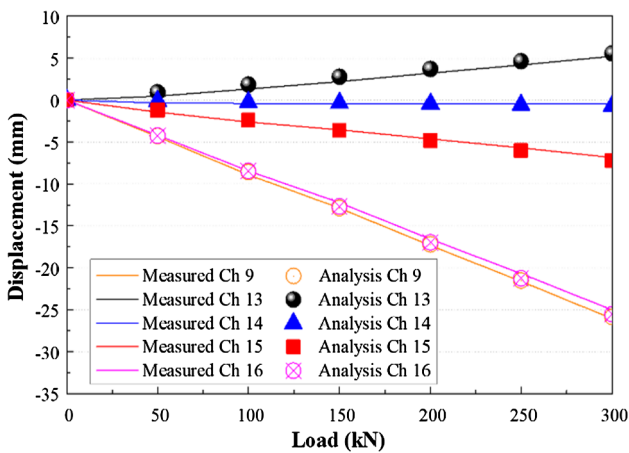
4.2. Displacement analysis of the rail fastening system

In this study, the experimental study was performed to confirm the behavior of the rail fastening system on the slab track at the railway bridge ends. The rail fastening system was considered as both linear and nonlinear stiffness models in the FEMs. The displacement results of the rail fastening system for the experimental and numerical models were determined by Eq. (1).

Fig. 10 shows a comparison of the experimental results and the finite-element analysis results for the girder ends. In Fig. 10(a), the upward displacement of the rail fastening system occurred mainly on the right side of the bridge abutment part, and the largest upward displacement occurred in the first rail fastening system at the bridge abutment part (i.e., rail fastening system 5). The nonlinear model



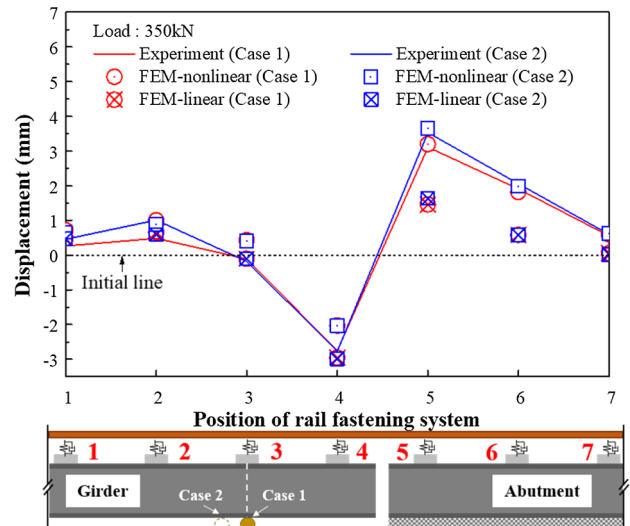
(a)



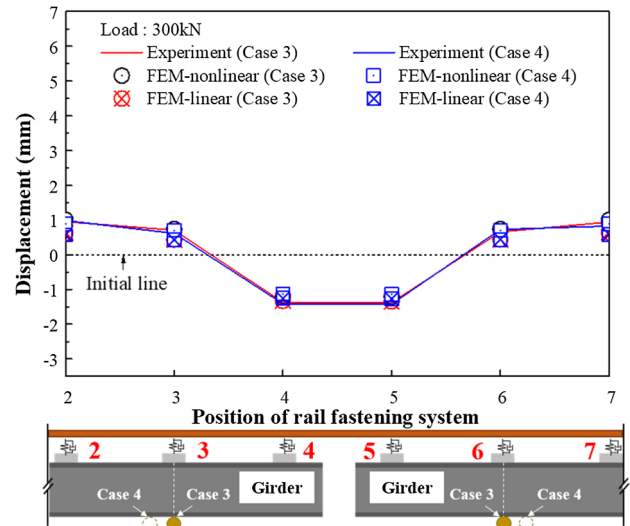
(b)

Fig. 8. Comparison of the experimental results and FEM results for the railway bridge models: (a) case 1; (b) case 3.

considering the actual rail fastening system exhibited closer results to the experiment than the linear model. The largest compressive displacement occurred in the last rail fastening system of the left girder (i.e., rail fastening system 4), and the maximum compressive displacement was 2 mm for the nonlinear model. This is because the compressive displacement of the nonlinear model was limited to 2 mm,

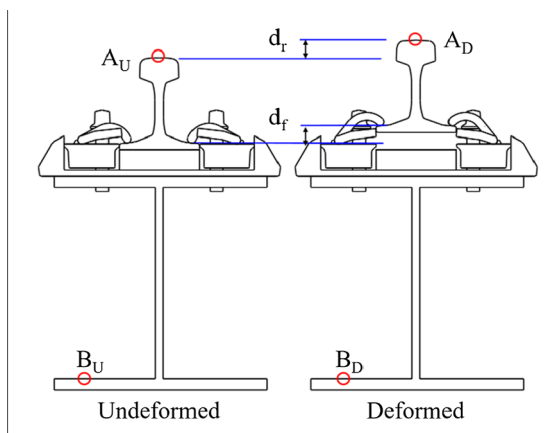


(a)

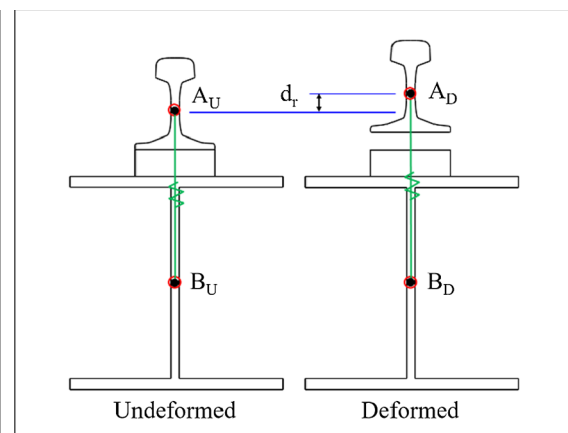


(b)

Fig. 10. Comparison of the experimental results and FEM results for the girder ends: (a) abutment model (load = 350 kN); (b) pier model (load = 300 kN).



(a)



(b)

Fig. 9. Assumptions for comparing the displacement results of the rail fastening system at the bridge ends: (a) experimental model; (b) numerical model.

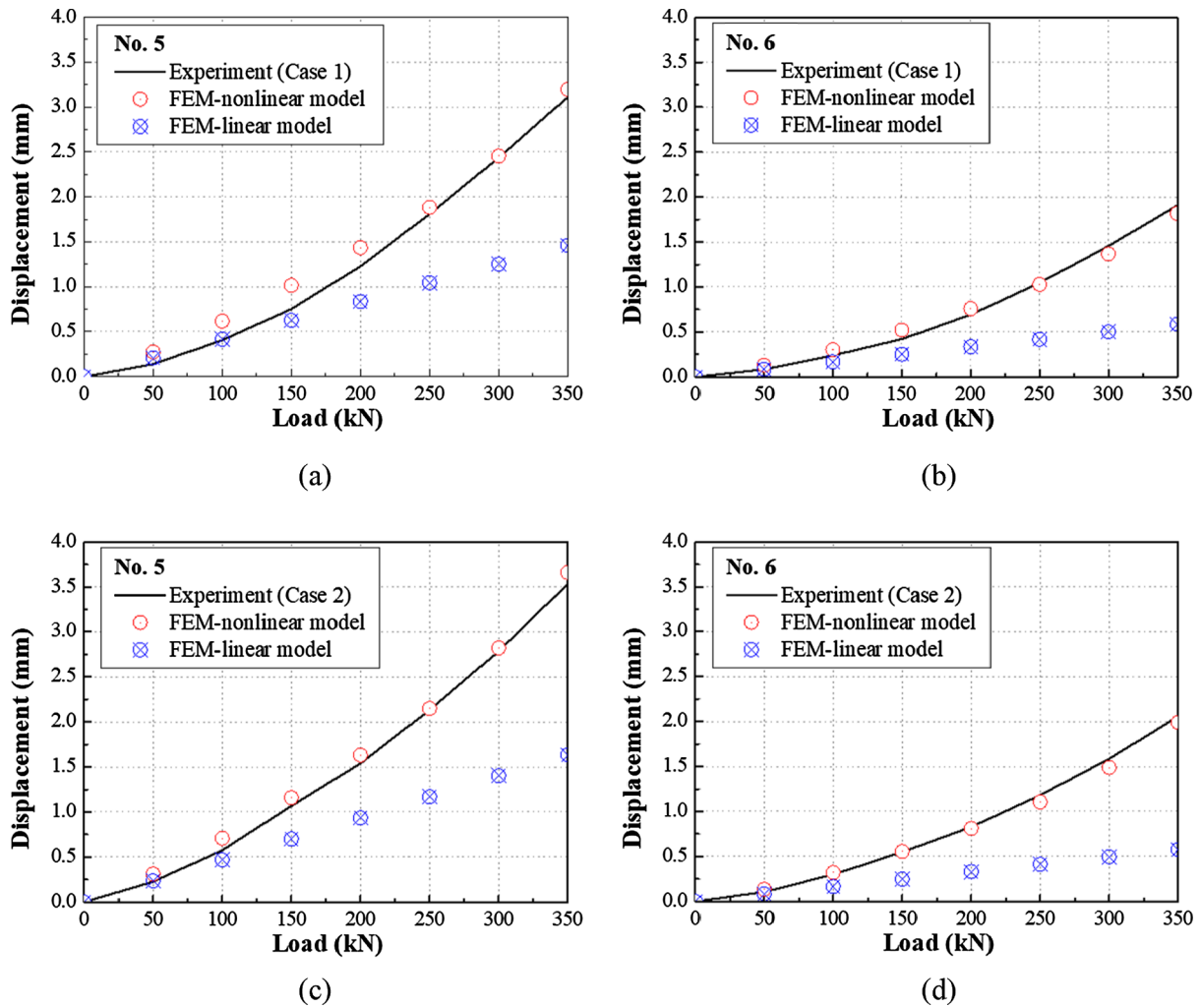


Fig. 11. Upward displacement of the rail fastening system in the abutment model: (a) position 5 of case 1; (b) position 6 of case 1; (c) position 5 of case 2; position 6 of case 2.

as shown in Fig. 6. In Fig. 10(b), symmetrical displacement responses in the case of the pier part appeared because the load was applied to the left and right girders simultaneously. Compressive displacement occurred in rail fastening systems 4 and 5, and upward displacement occurred at rail fastening systems 2, 3, 6, and 7.

Figs. 11 and 12 show the upward displacements of the rail fastening systems at the positions with large upward displacements, as shown in Fig. 10. In Fig. 11, the upward displacement of the rail fastening system in the experimental results is more similar to that for the nonlinear model than to that for the linear model. In Fig. 12, there was little difference between the results for the nonlinear and linear models because the displacement response was partially canceled out as the concentrated load was applied to the left and right girders, as shown in Fig. 10. Nevertheless, the upward displacement of the rail fastening system at the piers also indicates that the nonlinear model exhibited similar results to the experiment. In Fig. 12(a), the experimental results show negative displacements below 150 kN. This is because the negative displacement of the girder was larger than the negative displacement of the rail. The difference in slope at 150 kN in Fig. 12(c) occurred because the displacement of the rail was not measured up to 150 kN. Therefore, the nonlinear model of the rail fastening system simulated

the displacement response of the rail fastening system at the actual railway bridge ends more accurately than the linear model.

4.3. Analysis of force acting on the rail fastening system

The reaction force of the rail fastening system was investigated numerically. The reaction force of the rail fastening system in the abutment model and the pier model is shown in Figs. 13 and 14, respectively. Fig. 13 shows that the uplift force acting on the rail fastening system in the abutment model was smaller in the nonlinear model than in the linear model. In the case of the linear model, the uplift force was concentrated on the first rail fastening system (i.e., rail fastening system 5) of the abutment part. On the other hand, in the case of the nonlinear model, the uplift force seemed to be distributed to the rail fastening systems (i.e., rail fastening systems 5, 6, and 7) of the abutment part. Fig. 14 shows that there was no significant difference between the linear and nonlinear models of the rail fastening system in the pier part. This is mainly because the compressive force acted on the ends of the girder and the rail fastening system did not operate up to the plastic zone.

In the bridge abutment part, the uplift force acting on the rail

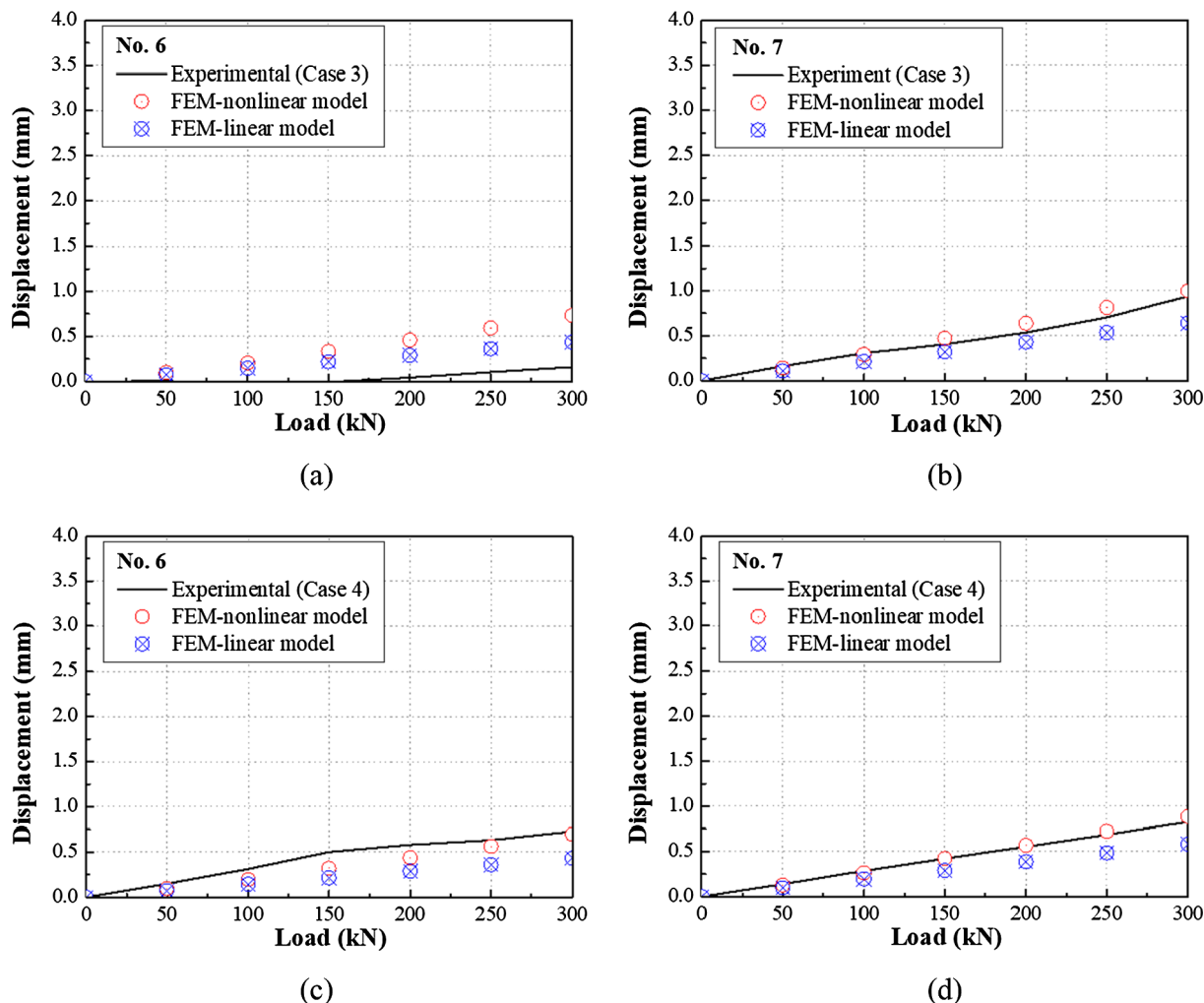


Fig. 12. Upward displacement of the rail fastening system in the pier model: (a) position 6 of case 3; (b) position 7 of case 3; (c) position 6 of case 4; position 7 of case 4.

fastening system 5 was increased when the position of the bridge support was away from the end of the girder (see Fig. 13(a) vs. (b)). However, in the bridge pier part, the compressive force acting on the rail fastening system 4 and 5 were reduced when the position of the bridge support was away from the end of the girder (see Fig. 14(a) vs. (b)). This indicates that the position of the bridge support is an important factor in evaluating the serviceability of the rail fastening system on the slab track at the railway bridge ends. By reducing the distance from the end of the girder to the bridge support, the force generated in the rail fastening system on the slab track at the railway bridge ends can be reduced. However, it should be noted that this can affect the dynamic behavior of the railway bridges by increasing the design length of the bridge.

Fig. 15 shows the simulated displacement and uplift force curve of the rail fastening system 5 in case 1 (i.e. abutment model). The black solid line indicates a load-displacement curve at the rail fastening system 5 by the experimental model (i.e. case 1). This was calculated by substituting the displacement measured at the rail fastening system 5 into the regression equation obtained from the clamping-force test (see Fig. 5(b)). The blue cross in a circle and the red-purple¹ circle marks represent the results obtained using the linear and nonlinear stiffness models, respectively. The serviceability evaluation of the slab track at

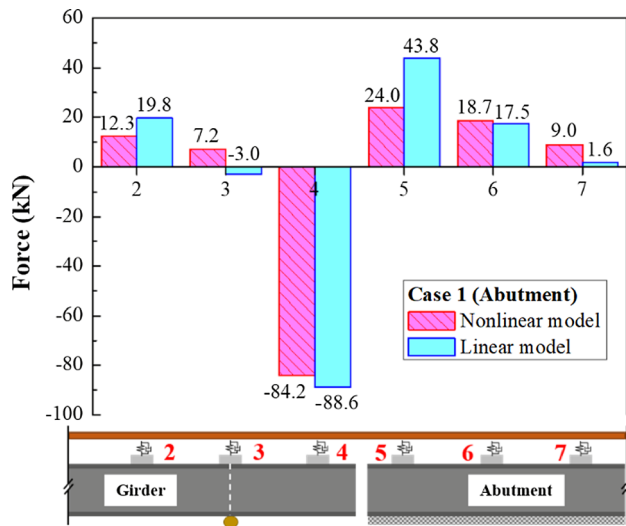
the railway bridge ends is based on the assumption that the rail fastening system is linear [8,9]. In the clamping-force test, the limit value of the uplift force of the KR-II rail fastening system was obtained as 20.19 kN (see Fig. 15). According to this limit value, the displacements of the linear and nonlinear stiffness models were 0.67 and 2.27 mm, respectively. Thus, the displacement was approximately 330% larger in the nonlinear stiffness model.

Even if the serviceability criteria [8,9] of the rail fastening system at the railway bridge ends is satisfied, the upward displacement can be larger than the design value of the rail fastening system, as shown in Fig. 15. Such large upward displacements occurring in the rail fastening systems at railway bridge ends may cause plastic deformation owing to the deviation of the rail fastening clip from the elastic region, resulting in severe damage.

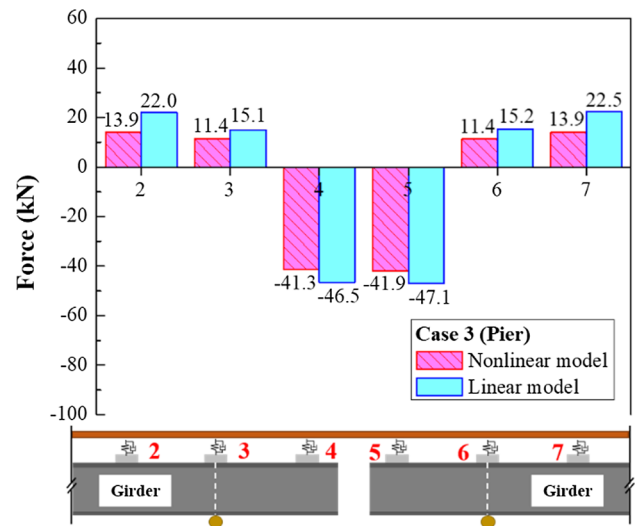
5. Conclusions

In this study, experimental and numerical studies have been carried out to investigate the behavior of the rail fastening system on slab track at the railway bridge ends. An experimental model test for the railway bridge ends and a clamping-force test for the rail fastening system were performed to verify the nonlinear behavior of the rail fastening system. Additionally, the finite-element analyses considering the rail fastening system as linear and nonlinear stiffness models were performed, and the results were compared with those of the model test. The following conclusions are drawn.

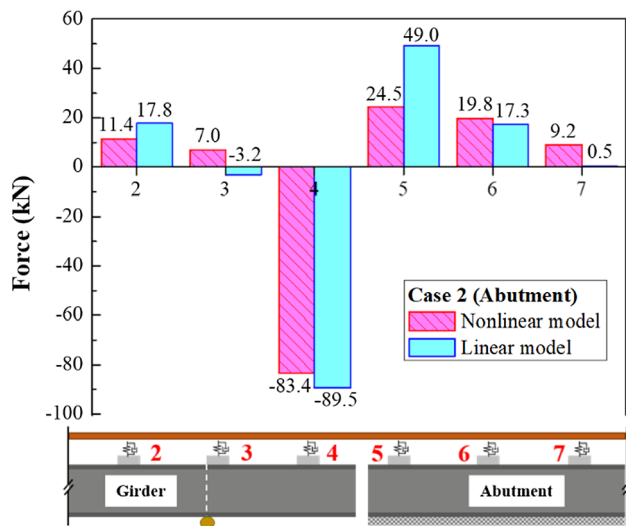
¹ For interpretation of color in Figs. 5 and 9, the reader is referred to the web version of this article.



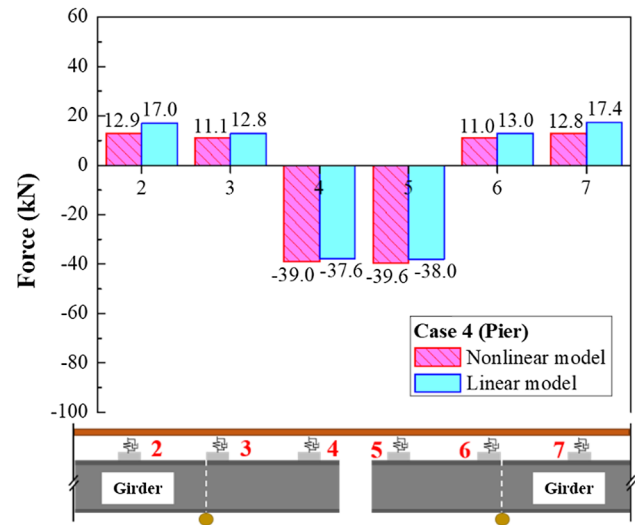
(a)



(a)



(b)



(b)

Fig. 13. Compression and uplift forces on the rail supports for each FEM in the abutment model (load = 350 kN): (a) case 1; (b) case 2.

- (1) The results of the finite-element analysis using the nonlinear stiffness model of the rail fastening system very well reflect the experimental results of the railway bridge. The nonlinear behavior of the rail fastening system is investigated as one of the main factors to be considered in the serviceability evaluation of rail fastening systems on the slab track at railway bridge ends.
- (2) The largest uplift force acts on the first rail fastening system of the bridge abutment part owing to the flexural behavior of the railway bridge. In the case of the linear model, the uplift force is concentrated on the first rail fastening system of the abutment part. On the other hand, in the case of the nonlinear model, the uplift force is distributed to the rail fastening systems of the abutment part.
- (3) The forces acting on the rail fastening system increase at the bridge abutment part and decrease at the bridge pier part when the

Fig. 14. Compression and uplift forces on the rail supports for each FEM in the pier model (load = 300 kN): (a) case 3; (b) case 4.

- position of the bridge support is away from the end of the girder.
- (4) When the rail fastening system is considered as a nonlinear stiffness model, the uplift displacement of the rail fastening system is considerably larger than that in the case of the linear stiffness model. Based on this conclusion it is proposed that in the field, a large displacement exceeding the allowable limit value owing to the nonlinear behavior of the rail fastening system can occur in the rail fastening system, even if the design of the slab track at the railway bridge ends is satisfied according to the current serviceability evaluation method.

The findings of this study indicate that it is necessary to employ the nonlinear behavior of the rail fastening system and investigate a displacement-based design method of the rail fastening system when evaluating the serviceability of the rail fastening system on the slab track at railway bridge ends.

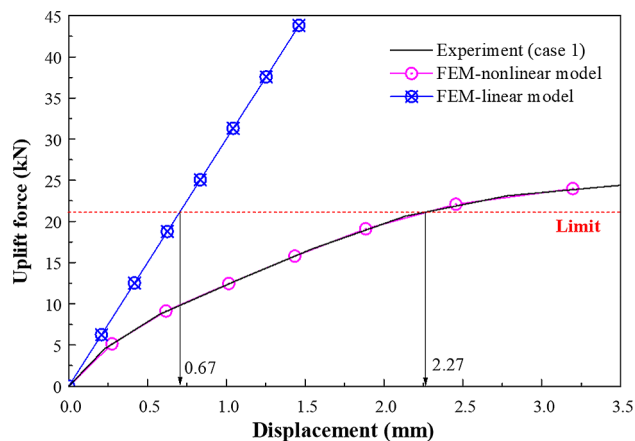


Fig. 15. Displacement and uplift force acting on the first rail fastening system in the abutment model.

Acknowledgments

This research was supported by a grant (18CTAP-C129908-02) from the Infrastructure and Transportation Technology Promotion Research Program, funded by the Ministry of Land, Infrastructure and Transport of the Korean Government.

Appendix A. Supplementary material

Supplementary data to this article can be found online at <https://doi.org/10.1016/j.engstruct.2019.05.098>.

References

- Kang C, Schneider S, Wenner M, Marx S. Development of design and construction of high-speed railway bridges in Germany. *Eng Struct* 2018;163:184–96.
- Union Internationale des Chemins de fer. High speed lines in the world. Paris: International Union of Railways; 2017.
- Yan B, Dai GL, Hu N. Recent development of design and construction of short span high-speed railway bridges in China. *Eng Struct* 2015;100:707–17.
- Gautier PE. Slab track: review of existing systems and optimization potentials including very high speed. *Constr Build Mater* 2015;92:9–15.
- Giannakos K. Deflection of a railway reinforced concrete slab track: comparing the theoretical results with experimental measurements. *Eng Struct* 2016;122:296–309.
- Moelter T. Closed and open joints for bridges on high speed lines. In: Calçada R, Delgado R, Matos AC, editors. *Bridges for high-speed railways*. London: CRC Press; 2008. p. 191–7.
- Gutierrez MJ, Edwards JR, Barkan CPL, Wilson B, Mediavilla J. Advancements in fastening system design for North American concrete crossties in heavy-haul service. Proceedings of AREMA annual conference, Orlando, USA. 2010.
- German Standard. DS804 Appendix 29. Bridge deck ends, check for serviceability limit state of superstructure. Regulation for railway bridges and other civil constructions. Berlin; 2008 [in German].
- Code, KR C-08090. Check for serviceability limit state of concrete track on bridge deck ends. Daejeon: Korea Rail Network Authority; 2014. [in Korean].
- Sañudo R, dell'Olivo L, Casado JA, Carrascal IA, Diego S. Track transition in railways: a review. *Constr Build Mater* 2016;112:140–57.
- Wang H, Markine V. Corrective countermeasure for track transition zones in railways: adjustable fastener. *Eng Struct* 2018;169:1–14.
- Paixão A, Fortunato E, Calçada R. Transition zones to railway bridges: track measurements and numerical modelling. *Eng Struct* 2014;80:435–43.
- Yang SC, Kim HH, Kong JS. Evaluation of uplift forces acting on fastening systems at the bridge deck end considering nonlinear behaviors of the fastening systems. *J Korean Soc Railw* 2017;20(4):521–8. [in Korean].
- Sung D. Nonlinear analysis method for serviceability investigation of bridge deck ends with a concrete slab track. *Adv Civil Eng* 2018;2018:6075686.
- Hess J. Rail expansion joints—the underestimated track work material? In: Calçada R, Delgado R, Matos AC, Goicolea JM, Gabaldon F, editors. *Track-bridge interaction on high-speed railways*. London: CRC Press; 2008. p. 149–64.
- Darr E, Fiebig W. *Feste fahrbahn: konstruktion und bauarten für eisenbahn und straßenbahn*. Hamburg (Germany): Eurailpress; 2006. [in German].
- Pfeifer RH, Molter TM. *Handbuch Eisenbahnbrücken*. Hamburg, Germany: DVV Media Group GmbH; 2008. [in German; Eurailpress].
- Park HK, Jang SY, Yang SC. A parametric study on the serviceability of concrete slab track on railway bridge. *J Korean Soc Railw* 2009;12(1):95–103. [in Korean].
- Pichler D, Fenske J. Ballastless track systems experiences gained in Austria and Germany. Proceedings of AREMA annual conference, Indianapolis, USA. 2013.
- Choi JH. Analysis of the internal forces of the rail supports for the serviceability of concrete slab track bridge. *J Korean Soc Civil Eng* 2013;33(4):1303–13. [in Korean].
- Choi JH. Influence of rail supporting spacing of railway bridge deck ends on bridge-track interaction forces. *J Korean Soc Railw* 2014;17(4):245–50. [in Korean].
- Lim JI, Song SO, Choi JY. Experimental study on characteristics of deformation for concrete track on railway bridge deck end induced by bridge end rotation. *J Korean Soc Railw* 2013;16(3):217–25. [in Korean].
- Turek J. Non-linear response of the track. *Veh Sys Dyn* 2007;24(1):265–79.
- Ruge P, Birk C. Longitudinal forces in continuously welded rails on bridge decks due to nonlinear track-bridge interaction. *Comput Struct* 2007;85:458–75.
- Chen Z, Shin M, Wei S, Andrawes B, Kuchama DA. Finite element modeling and validation of the fastening systems and concrete sleepers used in North America. *Proc Inst Mech Eng F J Rail Rapid Transit* 2014;228(6):590–602.
- Liu Y. Experimental and numerical analysis of nonlinear properties of rail fastening system [PhD. thesis]. Paris-Est University; 2015.
- Li QT, Luo Y, Liu Y. Estimating clamping force of rail fastener system by experimental and numerical methods. *Transp Res Proc* 2017;25:443–50.
- Oregui M, Li Z, Dollevoet R. An investigation into the modeling of railway fastening. *Int J Mech Sci* 2015;92:1–11.
- Zhao X, Li Z, Dollevoet R. Influence of the fastening modeling on the vehicle-track interaction at singular rail surface defects. *J Comput Nonl Dyn* 2014;9(3):031002.
- Luo Y, Liu Y, Yin H. Numerical investigation of nonlinear properties of a rubber absorber in rail fastening systems. *Int J Mech Sci* 2013;69:107–13.
- Fermer M, Nielsen JCO. Vertical interaction between train and track with soft and stiff railpads - full-scale experiments and theory. *Proc Inst Mech Eng F J Rail Rapid Transit* 1995;209(1):39–47.
- Hyundai steel. Product Guide - Part2. H Section. Available: <https://www.hyundai-steel.com/kr/products-technology/catalog/productcatalog1.hds> [accessed 15 May 2019] [in Korean].
- Hyundai steel. Railway rails. Available: <https://www.hyundai-steel.com/kr/products-technology/catalog/productcatalog3.hds> [accessed 15 May 2019] [in Korean].
- Korean Railway Standards. KRS TR 0001-15R. Rails. Uiwang: Korea Railroad Research Institute; 2006. [in Korean].
- Code, KRSA-T-2015-1005-R3. KR rail fastening system. Daejeon: Korea Rail Network Authority; 2017. [in Korean].
- Park S, Chang S, Sung D, Kwon S, Kim D. Behavior analysis of railway bridge deck ends according to rail support space and position of bridge bearing. *J Korean Soc Railw* 2019;22(4):328–35. [in Korean].
- Code, KR C-14060. Track material design. Daejeon: Korea Rail Network Authority; 2015. [in Korean].
- Han JG, Park SS, Kim WY. A study on the design specification of KR type rail fastening spring. Proceedings 2017 autumn conference of Korean Society for Railway, Hoengseong, Korea. 2017. p. 296–8. [in Korean].
- Nguyen VD, Lee CJ, Baek GH, Chang SK, Kim DK. The effect of nonlinear behaviour of the rail fastening system on the clamping forces in the railway bridge. Proceedings 2018 spring conference of Korea Institute for Structural Maintenance and Inspection, Jeju Island, Korea. 2018. p. 187–9. [in Korean].
- Tokyo Measuring Instruments Lab. High sensitive displacement transducer CDP. Available: <https://tml.jp/eng/documents/transducers/CDP.pdf> [accessed 15 May 2019].
- Computers and Structures, Inc., CSI analysis reference manual for SAP2000; 2017.
- Diego S, Casado JA, Carrascal I, Polanco JA, Gutiérrez-Solana F. Experimental validation of an adjustable railway fastening for slab track. *J Test Eval* 2010;38(5):598–608.
- Korean Railway Standards. KRS TR 0014-15R. Rail Fastening System. Uiwang: Korea Railroad Research Institute; 2009. [in Korean].
- European Committee for Standardization (CEN). EN 13146-7. Railway applications-Track. Test methods for fastening systems. Determination of clamping force (Part 7). Brussels; 2012.